

**Atomic origins of Si 2*p* and Au 4*f* surface core-level shifts on Au/Si(111)-(5 × 2)**

Se Gab Kwon and Myung Ho Kang\*

*Department of Physics, Pohang University of Science and Technology, Pohang 790-784, Korea*

(Received 6 August 2015; published 2 November 2015)

We have performed density functional theory calculations to investigate the core-level shifts on the Au/Si(111)-(5 × 2) surface. The employed structural model, which was recently proposed as containing seven Au atoms per (5 × 2) unit cell [*Phys. Rev. Lett.* **113**, 086101 (2014)], is found to well reproduce the Si 2*p* and Au 4*f* surface core-level shifts reported by previous x-ray photoelectron spectroscopy studies, thereby clarifying their atomic origins.

DOI: [10.1103/PhysRevB.92.195301](https://doi.org/10.1103/PhysRevB.92.195301)

PACS number(s): 68.43.Bc, 71.15.Mb, 81.07.Vb

**I. INTRODUCTION**

The Au/Si(111)-(5 × 2) surface is a representative, self-organized, one-dimensional metal-chain system, which has attracted great attention in surface physics since its first report in 1969 [1–14]. In particular, the construction of a correct structural model for the Au/Si(111)-(5 × 2) surface has been a central issue [15–22], but it was only recently that we finally reached a solid structural model. A density functional theory (DFT) study [23] provided a reliable structural model (see Fig. 1) that is energetically sound and well reproduces the experimental scanning tunneling microscopy (STM) images and angle-resolved photoemission spectra. This theoretical model was soon confirmed by the Patterson map analysis in a surface x-ray diffraction study [24] and was successfully used for analyzing the transmittance spectra in an infrared spectroscopy study [25].

In this paper, we use the recently proposed structural model [23] to theoretically investigate the Si 2*p* and Au 4*f* core-level shifts (CLSs) of the Au/Si(111)-(5 × 2) surface. In previous x-ray photoelectron spectroscopy (XPS) studies [26–28], the Si 2*p* and Au 4*f* core levels have been reported to reveal higher-binding-energy shifts relative to the bulk values, but their structural interpretation was given only qualitatively due to an absence of proper structural models. In what follows, we demonstrate by DFT calculations that the employed structural model [23] indeed well reproduces the measured Si 2*p* and Au 4*f* core levels [26–28], and their higher-binding surface shifts are consistent with the calculated charge redistribution at the surface.

**II. METHOD**

We perform DFT calculations using the Vienna *ab initio* simulation package [29] within the Perdew-Burke-Ernzerhof generalized gradient approximation [30] and the projector augmented wave method [31,32]. The CLS is calculated by using both initial- and final-state theories [33]. The initial-state shift is defined by the difference of the eigenvalues of a given core level at different local environments. The final-state shift, taking into account the core-hole screening effect, is calculated from the total energy difference of the systems with a core hole at different atomic sites. The Si(111) surface is modeled by a

periodic slab geometry with 12 atomic layers and a vacuum spacing of about 11 Å. We treat the (5 × 2) structure in an expanded (5 × 4) supercell in order to make the interaction of nearby core holes in the supercell negligible. The calculated value 2.372 Å is used as the bulk Si-Si bond length. Au atoms are adsorbed on the top of the slab, and the bottom of the slab is passivated by H atoms. We expand the electronic wave functions in a plane-wave basis with an energy cutoff of 250 eV. A (2 × 4 × 1) *k*-point mesh is used for the (5 × 4) Brillouin-zone integrations. All atoms but the bottom six Si layers are relaxed until the residual force components are within 0.02 eV/Å.

**III. RESULTS**

Figure 1 shows two structural models considered in the present CLS calculations. Figure 1(a) represents the *clean* Au/Si(111)-(5 × 2) surface [23], which features the Si honeycomb chains and the ×2 modulated Au chains. It is known that Si adatoms are always present in this surface, which tend to aggregate with ×4 spacing along the chain direction rather than uniformly distribute [34–36]. Figure 1(b) represents the saturated *Si-adatom* Au/Si(111)-(5 × 4) surface [23], where Si adatoms occupy hollow sites available within the Au chain and do not significantly affect the substrate structure. Here, we perform Si 2*p* and Au 4*f* CLS calculations for both of the clean (5 × 2) and Si-adatom (5 × 4) surfaces in order to compare with experimental data, where the actual amount of Si adatoms was unspecified [26–28].

**A. Si 2*p* core-level shifts**

Figure 2 shows the calculated Si 2*p* CLS for the clean and adatom surface models shown in Fig. 1. First, in the clean (5 × 2) surface, the core levels of the surface Si atoms are all shifted to the higher-binding-energy side. In the initial-state calculation, the shifts for the Si atoms *a*<sub>1</sub>–*a*<sub>4</sub> are marginal (0.02–0.14 eV), but those for the Si atoms *b*<sub>1</sub>–*b*<sub>4</sub> and *c*<sub>1</sub>–*c*<sub>4</sub> are substantial (0.51–0.73 eV). The final-state calculation moves the initial-state estimations toward the lower-binding-energy side by 0.17–0.51 eV, indicating that the surface core holes are more screened than the bulk ones because the screening effect tends to decrease the core-level binding energy [37,38].

The presence of Si adatoms is found to hardly change the Si 2*p* CLS of the clean surface in both initial- and final-state

\*kang@postech.ac.kr

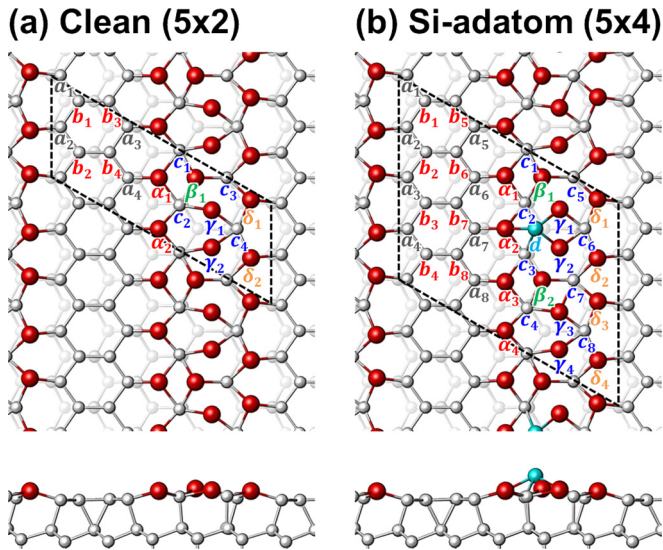


FIG. 1. (Color online) Atomic structures of (a) the clean Au/Si(111)-(5 × 2) surface and (b) the Si adsorbed Au/Si(111)-(5 × 4) surface. Large and small balls represent Au and Si atoms, respectively. Small and large dashed-line boxes represent the (5 × 2) and (5 × 4) unit cells, respectively. The surface Si (Au) atoms are labeled as  $a$ ,  $b$ ,  $c$ , and  $d$  ( $\alpha$ ,  $\beta$ ,  $\gamma$ , and  $\delta$ ) for later core-level resolutions.

calculations. The Si adatom itself does not even contribute a new prominent peak: Its core level (denoted as  $d$  in Fig. 2) overlaps with the core levels of the Si atoms  $b_1$ – $b_8$  and  $c_1$ – $c_8$ .

The bottom panel of Fig. 2 shows previous Si 2*p* XPS data. In early XPS studies [26,27], Okuda and co-workers resolved two Si 2*p* surface peaks ( $S_1$  and  $S_2$ ) in the higher-binding-energy side with an intensity ratio of about 11 to 1. Later, Zhang and co-workers [28] resolved one more surface peak ( $S'_1$ ) and attributed the peaks  $S_1$  and  $S'_1$  to two inequivalent types of Si dangling-bond atoms on the basis of earlier structural models [15,16] and the much weaker peak  $S_2$  to Si atoms related to surface defects. Our calculations indeed compare well with the XPS spectra in view that the initial- and final-state calculations could possibly represent the upper and lower bounds, respectively, of the experimental CLS [37,38]. From the comparison with calculations, the atomic origins of the XPS peaks can be clarified as follows. First, the main peak  $S_1$  is evidently attributed to the Si atoms  $b_1$ – $b_4$  and  $c_1$ – $c_4$  of the clean surface and the Si atoms  $b_1$ – $b_8$ ,  $c_1$ – $c_8$ , and  $d$  of the Si-adatom surface. Second, the origin of the peak  $S'_1$  is twofold: We may regard it as a tail part of the peak  $S_1$ , contributed from some of the above-mentioned Si atoms showing slightly lower-binding shifts, but it is also possible that it represents the Si atoms  $a_1$ – $a_4$  of the clean surface and  $a_1$ – $a_8$  of the Si-adatom surface, although they seem to contribute more to the bulk peak. Finally, the binding energy of the weak component  $S_2$  shows a difference of about 0.2 eV between the two experiments, which marginally overlaps at about 0.8 eV with the upper end of the calculated binding energies. We suspect it as a Si-adatom-induced weak feature: As seen in our calculations, some Si atoms undergo slightly more higher-binding shifts by the presence of Si adatoms (i.e., the core levels  $c_2$  and  $c_3$  of the Si-adatom surface). Of course, the early interpretation as

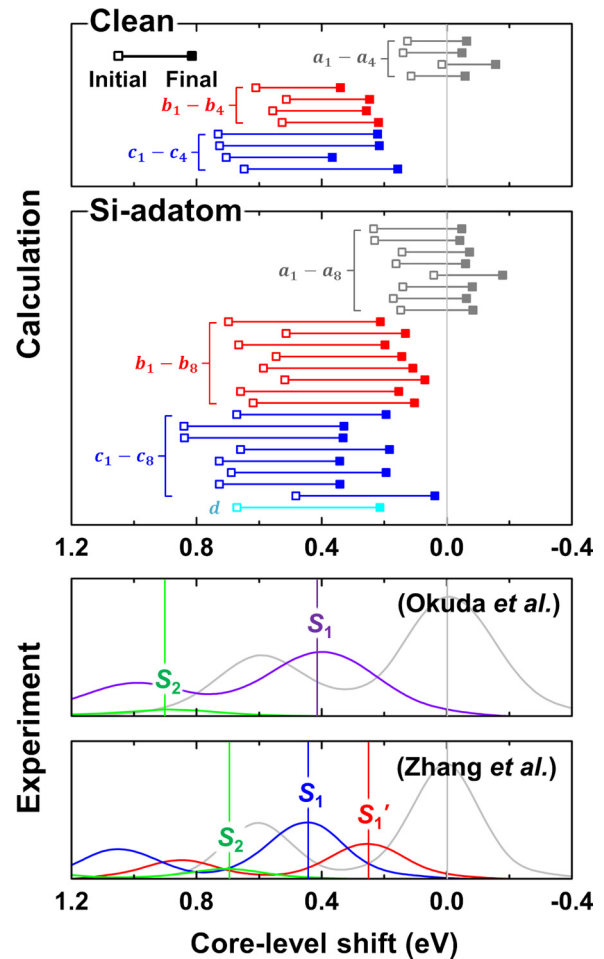


FIG. 2. (Color online) Si 2*p* core-level shifts. The labels ( $a$ ,  $b$ ,  $c$ , and  $d$ ) indicate their atomic origins as marked in Fig. 1. The core levels are given relative to the bulk value that is effectively estimated from the atoms in the fifth and sixth Si layers. Experimental data were adapted from the work of Okuda and co-workers [26,27] and Zhang and co-workers [28].

a defect-related origin [28] is not ruled out, but we think that the peak intensity of  $S_2$  is too strong to be considered a surface defect (the reported intensity as large as about 10% of  $S_1 + S'_1$  could imply about one defect-related Si atom per 5 × 2 unit cell).

Figure 3 shows the electronic charge around the surface Si atoms relative to the bulk value, which well accounts for the higher-binding surface shifts of the Si 2*p* core levels. The overall depletion of the valence charge at the surface Si atoms results in a weaker Coulomb repulsion between the core and valence electrons, thereby leading to a higher-binding shift of the core level. We find that the magnitude of the CLS is in line with the amount of depletion of the total charge. The charge depletion at around the surface Si atoms indicates a charge transfer from Si to Au atoms. Thus, the present charge analysis confirms the previous qualitative argument given by Okuda and co-workers [26,27] that a charge transfer from Si to more electronegative Au atoms is responsible for the higher-binding Si 2*p* CLS.

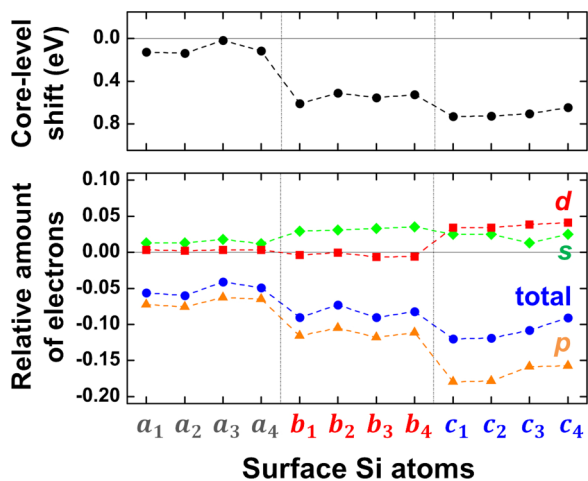


FIG. 3. (Color online) Electronic-charge analysis of the Si 2*p* CLS. The top panel shows the initial-state Si 2*p* CLS of the clean surface (see Fig. 2). The bottom panel shows the amount of electrons around the surface Si atoms: The total charge and its *s*, *p*, and *d* components are given relative to the bulk values. The electron counting was done by using an atomic radius of 1.26 Å, which represents half of the average Au-Si bond length in the clean ( $5 \times 2$ ) surface.

### B. Au 4*f* core-level shifts

Figure 4 shows the calculated Au 4*f* CLS for the clean and adatom surface models shown in Fig. 1. In the clean ( $5 \times 2$ ) surface, the initial-state calculations show overall higher-binding shifts (0.21–0.90 eV) for the surface Au atoms, and the final-state calculations result in slightly more increased binding energies (by 0.06–0.12 eV, except for the level  $\alpha_2$ ), implying that the surface Au atoms are less screened than the bulk ones. The average values of +0.47 eV (initial state) and +0.54 eV (final state) compare well with the XPS measurement by Okuda and co-workers [26,27] that resolved only one surface peak at about +0.5 eV.

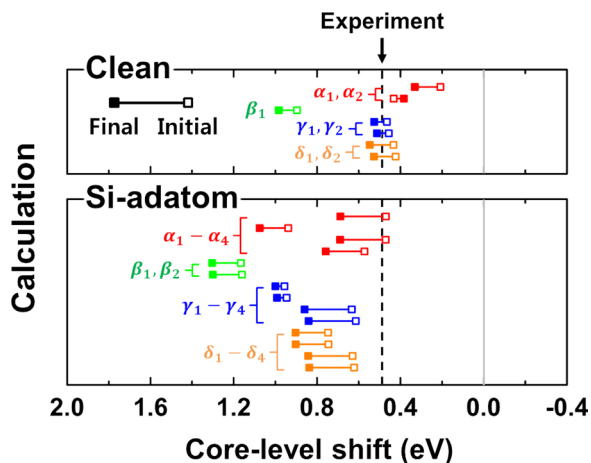


FIG. 4. (Color online) Au 4*f* core-level shifts. The labels ( $\alpha$ ,  $\beta$ ,  $\gamma$ , and  $\delta$ ) indicate their atomic origins as marked in Fig. 1. The core levels are given relative to the bulk value of fcc Au. Dashed lines represent the experimental value reported by Okuda and co-workers [26,27].

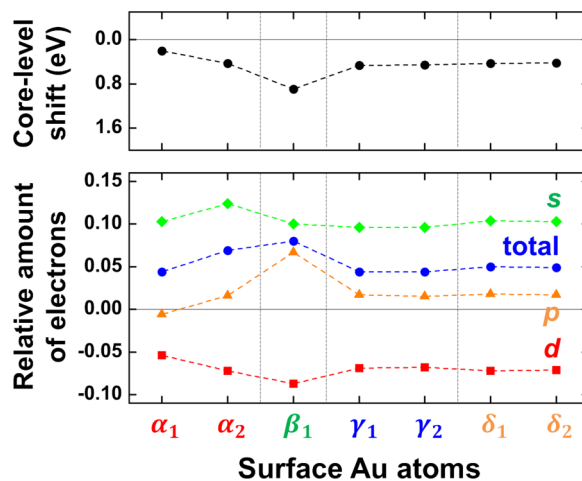


FIG. 5. (Color online) Electronic-charge analysis of the Au 4*f* CLS. The top panel shows the initial-state Au 4*f* CLS of the clean surface (see Fig. 4). The bottom panel shows the amount of electrons around the Au atoms: The total charge and its *s*, *p*, and *d* components are given relative to the bulk values of fcc Au. The same atomic radius 1.26 Å was used for the electron countings.

The bottom panel of Fig. 4 shows that the presence of Si adatoms has a noticeable effect on the Au 4*f* core levels of the clean surface, leading to more higher-binding shifts by about 0.1–0.5 eV. This effect is compatible with the previous DFT report [23] that the Si adatoms are in a partially ionized state by donating electrons to the Au/Si(111)-( $5 \times 2$ ) surface: Such positively ionized Si adatoms would lower the core levels of nearby Au atoms via Coulomb attractions, as is evident in our calculations that the core levels of the nearest Au atoms (i.e.,  $\alpha_2$ ,  $\beta_1$ ,  $\beta_2$ ,  $\gamma_1$ , and  $\gamma_2$ ) underwent larger shifts. As a result, the average values of +0.76 eV (initial state) and +0.93 eV (final state) of the Si-adatom surface somewhat overestimate the XPS data of about +0.5 eV [26,27].

Finally, let us figure out why the Au 4*f* core level undergoes a higher-binding surface shift: It is interesting in view that the aforementioned charge transfer from Si to Au atoms implies a lower-binding surface shift instead. Figure 5 displays the electronic charge around the surface Au atoms relative to the bulk value. The total charges are certainly increased, but we find that the large increase in 6*s* and 6*p* electrons is greatly offset by a substantial decrease in 5*d* electrons, and the higher-binding Au 4*f* CLSs are almost in line with the decreases in 5*d* electrons. This indicates that, since the more localized 5*d* electrons exert a much stronger Coulomb repulsion on the core, the energy gain by their depletion dominates the energy loss by the increase in 6*s* and 6*p* electrons. Therefore, our orbital-resolved electronic-charge analysis directly confirms the previous experimental interpretation by Okuda and co-workers [26,27], where a depletion of *d* electrons at the Au atoms was inferred from the higher-binding Au 4*f* CLSs measured on this surface.

## IV. SUMMARY

The present DFT calculations on the recently proposed structural model [23] for the Au/Si(111)-( $5 \times 2$ ) surface well

reproduced the experimentally reported Si  $2p$  and Au  $4f$  core-level shifts, thereby clarifying their atomic origins. In our quantitative electron-counting analysis, the higher-binding shifts of Si  $2p$  and Au  $4f$  core levels were attributed to a charge transfer from Si to Au atoms and a depletion of  $d$  electrons at the Au atoms, respectively, in support of earlier experimental interpretations.

*Note added.* We extended our CLS calculations for the earlier Erwin-Barke-Himpsel (EBH) model [21] and found

that, with similar core-level shifts to the present Kwon-Kang (KK) model [23], the EBH model is also compatible with the CLS experiments (see the Supplemental Material [39]).

#### ACKNOWLEDGMENT

This work was supported by the National Research Foundation of Korea (Grant No. 2011-0008907).

- 
- [1] H. E. Bishop and J. C. Rivière, Segregation of gold to the silicon (111) surface observed by Auger emission spectroscopy and by LEED, *J. Phys. D* **2**, 1635 (1969).
- [2] H. Lipson and K. E. Singer, Disorder in a film of gold deposited on silicon: Investigation by low-energy electron diffraction, *J. Phys. C* **7**, 12 (1974).
- [3] G. LeLay and J. P. Faurie, AES study of the very first stages of condensation of gold films on silicon (111) surfaces, *Surf. Sci.* **69**, 295 (1977).
- [4] C. Schamper, W. Moritz, H. Schulz, R. Feidenhans'l, M. Nielsen, F. Grey, and R. L. Johnson, Static lattice distortions and the structure of Au/Si(111)-(5 × 1): An x-ray-diffraction study, *Phys. Rev. B* **43**, 12130 (1991).
- [5] J. D. O'Mahony, C. H. Patterson, J. F. McGilp, F. M. Leible, P. Weightman, and C. F. J. Flipse, The Au-induced 5 × 2 reconstruction on Si(111), *Surf. Sci.* **277**, L57 (1992).
- [6] I. R. Collins, J. T. Moran, P. T. Andrews, R. Cosso, J. D. O'Mahony, J. F. McGilp, and G. Margaritondo, Angle-resolved photoemission from an unusual quasi-one-dimensional metallic system: a single domain Au-induced 5 × 2 reconstruction of Si(111), *Surf. Sci.* **325**, 45 (1995).
- [7] R. Losio, K. N. Altmann, and F. J. Himpsel, Continuous Transition From Two- to One-Dimensional States in Si(111)-(5 × 2)-Au, *Phys. Rev. Lett.* **85**, 808 (2000).
- [8] M.-H. Kang and J. Y. Lee, Theoretical investigation of the Au/Si(111)-(5 × 2) surface structure, *Surf. Sci.* **531**, 1 (2003).
- [9] H. S. Yoon, S. J. Park, J. E. Lee, C. N. Whang, and I.-W. Lyo, Novel Electronic Structure of Inhomogeneous Quantum Wires on a Si Surface, *Phys. Rev. Lett.* **92**, 096801 (2004).
- [10] E. Bussmann, S. Bockenhauer, F. J. Himpsel, and B. S. Swartzentruber, One-Dimensional Defect-Mediated Diffusion of Si Adatoms on the Si(111)-(5 × 2)-Au Surface, *Phys. Rev. Lett.* **101**, 266101 (2008).
- [11] N. McAlinden and J. F. McGilp, New evidence for the influence of step morphology on the formation of Au atomic chains on vicinal Si(111) surfaces, *Europhys. Lett.* **92**, 67008 (2010).
- [12] I. Barke, S. Polei, V. v. Oeynhausen, and K.-H. Meiwes-Broer, Confined Doping on a Metallic Atomic Chain Structure, *Phys. Rev. Lett.* **109**, 066801 (2012).
- [13] C. Hogan, E. Ferraro, N. McAlinden, and J. F. McGilp, Optical Fingerprints of Si Honeycomb Chains and Atomic Gold Wires on the Si(111)-(5 × 2)-Au Surface, *Phys. Rev. Lett.* **111**, 087401 (2013).
- [14] J. Kautz, M. W. Copel, M. S. Gordon, R. M. Tromp, and S. J. van der Molen, Titration of submonolayer Au growth on Si(111), *Phys. Rev. B* **89**, 035416 (2014).
- [15] L. D. Marks and R. Plass, Atomic Structure of Si(111)-(5 × 2)-Au from High Resolution Electron Microscopy and Heavy-Atom Holography, *Phys. Rev. Lett.* **75**, 2172 (1995).
- [16] T. Hasegawa, S. Hosaka, and S. Hosoki, Domain growth of Si(111)-5 × 2 Au by high-temperature STM, *Surf. Sci.* **357**, 858 (1996).
- [17] S. C. Erwin, Self-Doping of Gold Chains on Silicon: A New Structural Model for Si(111)-(5 × 2)-Au, *Phys. Rev. Lett.* **91**, 206101 (2003).
- [18] S. Riikonen and D. Sánchez-Portal, First-principles study of the atomic and electronic structure of the Si(111)-(5 × 2)-Au surface reconstruction, *Phys. Rev. B* **71**, 235423 (2005).
- [19] C.-Y. Ren, S.-F. Tsay, and F.-C. Chuang, First-principles study of the atomic and electronic structure of the Si(111)-(5 × 2)-Au surface reconstruction, *Phys. Rev. B* **76**, 075414 (2007).
- [20] F.-C. Chuang, C.-H. Hsu, C.-Z. Wang, and K.-M. Ho, Honeycomb chain structure of the Au/Si(111)-(5 × 2) surface reconstruction: A first-principles study, *Phys. Rev. B* **77**, 153409 (2008).
- [21] S. C. Erwin, I. Barke, and F. J. Himpsel, Structure and energetics of Si(111)-(5 × 2)-Au, *Phys. Rev. B* **80**, 155409 (2009).
- [22] T. Abukawa and Y. Nishigaya, Structure of the Si(111)-(5 × 2)-Au Surface, *Phys. Rev. Lett.* **110**, 036102 (2013).
- [23] S. G. Kwon and M. H. Kang, Identification of the Au Coverage and Structure of the Au/Si(111)-(5 × 2) Surface, *Phys. Rev. Lett.* **113**, 086101 (2014).
- [24] T. Shirasawa, W. Voegeli, T. Nojima, Y. Iwasawa, Y. Yamaguchi, and T. Takahashi, Identification of the Structure Model of the Si(111)/(5 × 2)-Au Surface, *Phys. Rev. Lett.* **113**, 165501 (2014).
- [25] F. Hötzel, K. Seino, C. Huck, O. Skibbe, F. Bechstedt, and A. Pucci, Metallic properties of the Si(111)-(5 × 2)-Au surface from infrared plasmon polaritons and *ab initio* theory, *Nano Lett.* **15**, 4155 (2015).
- [26] T. Okuda, H. Daimon, H. Shigeoka, S. Suga, T. Kinoshita, and A. Kakizaki, Surface core level shifts of the Au adsorbed Si(111) reconstructed surfaces, *J. Electron Spectrosc. Relat. Phenom.* **80**, 229 (1996).
- [27] T. Okuda, H. Daimon, S. Suga, Y. Tezuka, and S. Ino, Surface electronic structure of ordered alkali- and noble metal-overlayers on Si(111), *Appl. Surf. Sci.* **121-122**, 89 (1997).
- [28] H. M. Zhang, T. Balasubramanian, and R. I. G. Uhrberg, Core-level photoelectron spectroscopy study of the Au/Si(111) 5 × 2,  $\alpha\text{-}\sqrt{3} \times \sqrt{3}$ ,  $\beta\text{-}\sqrt{3} \times \sqrt{3}$ , and 6 × 6 surfaces, *Phys. Rev. B* **65**, 035314 (2001).

- [29] G. Kresse and J. Furthmüller, Efficient iterative schemes for *ab initio* total-energy calculations using a plane-wave basis set, *Phys. Rev. B* **54**, 11169 (1996).
- [30] J. P. Perdew, K. Burke, and M. Ernzerhof, Generalized gradient approximation made simple, *Phys. Rev. Lett.* **77**, 3865 (1996).
- [31] P. E. Blöchl, Projector augmented-wave method, *Phys. Rev. B* **50**, 17953 (1994).
- [32] G. Kresse and D. Joubert, From ultrasoft pseudopotentials to the projector augmented-wave method, *Phys. Rev. B* **59**, 1758 (1999).
- [33] L. Köhler and G. Kress, Density functional study of CO on Rh(111), *Phys. Rev. B* **70**, 165405 (2004).
- [34] R. Bennewitz, J. N. Crain, A. Kirakosian, J.-L. Lin, J. L. McChesney, D. Y. Petrovykh, and F. J. Himpsel, Atomic scale memory at a silicon surface, *Nanotechnology* **13**, 499 (2002).
- [35] A. Kirakosian, J. N. Crain, J.-L. Lin, J. L. McChesney, D. Y. Petrovykh, F. J. Himpsel, and R. Bennewitz, Silicon adatoms on the Si(111)5 × 2-Au surface, *Surf. Sci.* **532-535**, 928 (2003).
- [36] W. H. Choi, P. G. Kang, K. D. Ryang, and H. W. Yeom, Band-structure engineering of gold atomic wires on silicon by controlled doping, *Phys. Rev. Lett.* **100**, 126801 (2008).
- [37] E. Pehlke and M. Scheffer, Evidence for site-sensitive screening of core holes at the Si and Ge(001) surface, *Phys. Rev. Lett.* **71**, 2338 (1993).
- [38] M. Kuzmin, M. J. P. Punkkinen, P. Laukkanen, J. J. K. Lång, J. Dahl, M. Tuominen, V. Tuominen, J. Adell, T. Balasubramanian, L. Vitos, and K. Kokko, Dimer-T<sub>3</sub> reconstruction of the Sm/Si(100)(2 × 3) surface studied by high-resolution photoelectron spectroscopy and density functional theory calculations, *Phys. Rev. B* **84**, 245322 (2011).
- [39] See Supplemental Material at <http://link.aps.org/supplemental/10.1103/PhysRevB.92.195301> for additional CLS calculations.